Supplementary Information

B2-structured indium–platinum group metal high-entropy intermetallic nanoparticles

Masashi Nakamura,[a] Dongshuang Wu,*[a] Megumi Mukoyoshi,[a] Kohei Kusada,[a,b] Takaaki Toriyama,[c] Tomokazu Yamamoto,[c] Syo Matsumura,[d] Yasukazu Murakami,[c,e] Shogo Kawaguchi,[f] Yoshiki Kubota[g] and Hiroshi Kitagawa*[a]

a. Division of Chemistry, Graduate School of Science, Kyoto University, Kitashirakawa-Oiwakecho, Sakyo-ku, Kyoto 606-8502, Japan

b. The HAKUBI Center for Advanced Research, Kyoto University, Kitashirakawa-Oiwakecho, Sakyo-ku, Kyoto 606-8502, Japan

c. The Ultramicroscopy Research Center, Kyushu University, 744 Motooka, Nishi-ku, Fukuoka 819-0395, Japan

d. National Institute of Technology, Kurume College, 1-1-1 Komorino, Kurume, Fukuoka 830-8555, Japan

e. Department of Applied Quantum Physics and Nuclear Engineering, Graduate School of Engineering, Kyushu University, 744 Motooka, Nishi-ku, Fukuoka 819-0395, Japan

f. Japan Synchrotron Radiation Research Institute (JASRI), SPring-8, 1-1-1 Kouto, Sayo-cho, Sayo-gun, Hyogo 679-5198, Japan

g. Department of Physics, Graduate School of Science, Osaka Metropolitan University, 1-1 Gakuen-cho, Naka-ku, Sakai, Osaka 599-8531, Japan

E-mails

Dongshuang Wu : dongshuang.wu@ntu.edu.sg

Hiroshi Kitagawa : kitagawa@kuchem.kyoto-u.ac.jp

▼Experimental Details

Synthesis of PNPs

PNPs were synthesised by a wet-chemistry method using polyol solvent. First, three solutions, respectively containing metal precursors, a reducing agent and a protecting agent, were prepared. As metal precursors, the following chemicals were selected: indium(III) chloride tetrahydrate ($InCl_3 \cdot 4H_2O$, Nacalai Tesque, Japan), iridium acetate ($Ir(CH_3COO)_n$, Wako, Japan), rhodium(III) chloride trihydrate ($RhCl_3 \cdot 3H_2O$, Wako, Japan), ruthenium(III) chloride trihydrate ($RuCl_3 \cdot 3H_2O$, Wako, Japan), palladium(II) bis(acetylacetonate) ($Pd(C_5H_7O_2)_2$, Wako, Japan) and potassium tetrachloroplatinate(II) (K_2PtCl_4, Wako, Japan). The total molar amount of the precursors was 0.60 mmol, consisting of 0.30 mmol of indium salt and 0.06 mmol of each PGM salt. The precursors were dissolved in the mixture of TEG (12.5 mL, TCI, Japan) and dibenzyl ether (2.5 mL, TCI, Japan). The reducing agent, $NaBH_4$ (9.0 mmol, Wako, Japan), was dissolved in TEG (25 mL). Because $NaBH_4$ gradually decomposes in a protic solvent like TEG, this solution was quickly prepared just before use. In addition, PVP (K30, 12 mmol in monomeric unit, Wako, Japan), a protecting agent, was dissolved in 60 mL of TEG, and then heated to 200 °C under Ar atmosphere. Then, the metal precursor solution and the reducing agent solution were concurrently injected into the preheated protecting agent solution at the rate of 1.0 mL/min. At high temperature, much of $NaBH_4$ would be decomposed without performing its reducing agent function, so 5 mL of the reducing agent solution was added before starting the co-injection, and the other 5 mL of the reducing agent solution was continuously injected even after completing the injection of the metal precursor solution. Afterwards, the solution was rapidly cooled down to RT in an ice-water bath. The obtained black-coloured solution was mixed with moderate amounts of ethanol, acetone and diethyl ether and centrifuged several times at 7830 rpm to separate the NPs as black-coloured powders.

X-ray fluorescence spectroscopy (XRF)

The composition of the PNPs were measured using a ZSX PrimusIV (Rigaku, Japan). The results are shown in Fig. S1.

Transmission electron microscopy (TEM)

The microscopic images of the samples were obtained using an HT7700 (Hitachi, Japan) with an acceleration voltage of 100 kV. Fig. S2 shows the TEM images of PNPs, and Fig. S3 shows the images of PNPs/C and In–PGM HEI NPs/C.

In-situ synchrotron PXRD

In-situ synchrotron PXRD measurements were performed at SPring-8, beamline BL02B2 at an incident X-ray wavelength of 0.63 Å. The PNPs were placed into a glass capillary (borosilicate, W. Müller, Germany) and an additional thinner capillary was inserted to avoid scattering of the powders. The capillary was then mounted on the goniometer head connected with pumps and an H_2 gas cylinder. First, the capillary was evacuated, and subsequently, 1 atm of H_2 was introduced. In the heating process, the temperature was controlled by spraying heated N_2 gas. The PXRD patterns were acquired at seven different temperatures (RT (30 °C), 100, 200, 300, 400, 500 and 600 °C). The heating rate was 80 K/min and a waiting time of 30 s was set after reaching the target temperature before the PXRD data acquisition. After the maximum temperature, the sample was evacuated and cooled to RT, and finally, the PXRD pattern of the resultant HEI NPs was acquired.

Preparation of PNPs/C and In–PGM HEI NPs/C

Because as-synthesised PNPs were often found to be aggregated in the TEM images (Fig. S2), PNPs loaded on carbon (PNPs/C) were prepared for observation by STEM. After the NPs were physically mixed with carbon (VXC72R, Cabot Corp., USA) for 20 min, the mixture was dispersed in ethanol and sonicated for 1 h. Finally, PNPs/C were collected by centrifugation. Then, In–PGM HEI NPs/C were prepared by the heat treatment of PNPs/C. PNPs/C were placed in a glass tube and the air inside was replaced with 1 atm of H_2. The tube was heated at 350 °C in a mantle heater for 20 min, and then gradually cooled to RT to obtain In–PGM HEI NPs/C. The TEM images and PXRD patterns of PNPs/C and In–PGM HEI NPs/C are shown in Figs. S3 and S4, respectively.

Scanning-transmission electron microscopy (STEM)

The STEM images of PNPs/C and In–PGM HEI NPs/C were acquired using a JEM-ARM200CF instrument (JEOL, Japan) at the Ultramicroscopy Research Center, Kyushu University. The acceleration voltage was 120 kV. The HAADF images are shown in Fig. S5 (PNPs/C), Fig. 2 and Fig. S6 (In–PGM HEI NPs/C). In addition, spatially resolved EDX analysis was performed using the EDX spectrometer attached to the microscope. The atomic-resolution maps and line profile of In–PGM HEI NPs/C are shown in Fig. 2 and Fig. 3, respectively.

Lab-source PXRD

The lab-source PXRD patterns were acquired with a MiniFlex600 (Rigaku, Japan) using Cu$K\alpha$ radiation as an incident X-ray beam. The PXRD patterns of PNPs/C and In–PGM HEI NPs/C (Fig. S4) were measured by the lab-source PXRD.

▼General characterisation of wet-chemically synthesised NPs

XRF

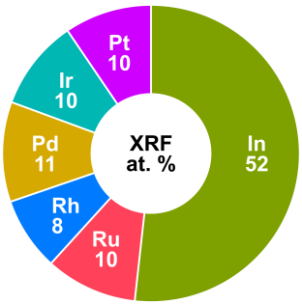

Fig. S1 Compositions (at.%) of PNPs determined by XRF.

TEM

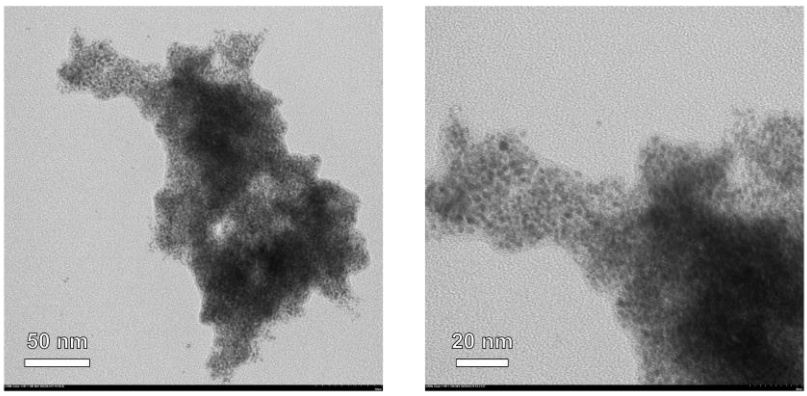

Fig. S2 TEM images of PNPs. Both images show the same region of interest but at different magnifications.

▼Rietveld analysis of synchrotron *in-situ* PXRD of PNPs

The synchrotron PXRD patterns were analysed by Rietveld refinement using GSAS-II software. The profile parameters were calibrated by CeO_2 standard possessed by the beamline. For example, the wavelength was determined to be 0.630407(1) Å. The model structures were set according to the compositions determined by XRF as a simple approximation (Table S1) (although the macroscopic composition in XRF might not be equivalent to the compositions of the crystalline parts because the amorphous components were observed in the STEM images). The backgrounds were estimated based on the diffraction pattern from the blank capillary at the same temperature. The results of the Rietveld refinement are given in Fig. 1b and Table 1 in the main article.

Table S1 The model crystal structure used to perform Rietveld analysis of (a) PNPs (*Fm*-3*m*, A1 (fcc)) and (b) In–PGM HEI NPs (*Pm*-3*m*, B2). Each column indicates the Wyckoff position, site symmetry, fractional coordinates, atom and occupancy of the crystallographic sites, respectively.

(a)

Wyckoff	Symm.	*x*	*y*	*z*	Atom	Occ.
4a	*m*-3*m*	0	0	0	In	0.518
					Ru	0.100
					Rh	0.080
					Pd	0.109
					Ir	0.099
					Pt	0.095

(b)

Wyckoff	Symm.	*x*	*y*	*z*	Atom	Occ.
1a	*m*-3*m*	0	0	0	In	1.000
1b	*m*-3*m*	0.5	0.5	0.5	Ru	0.207
					Rh	0.166
					Pd	0.226
					Ir	0.205
					Pt	0.197

▼General characterisation of PNPs/C and In–PGM HEI NPs/C

TEM

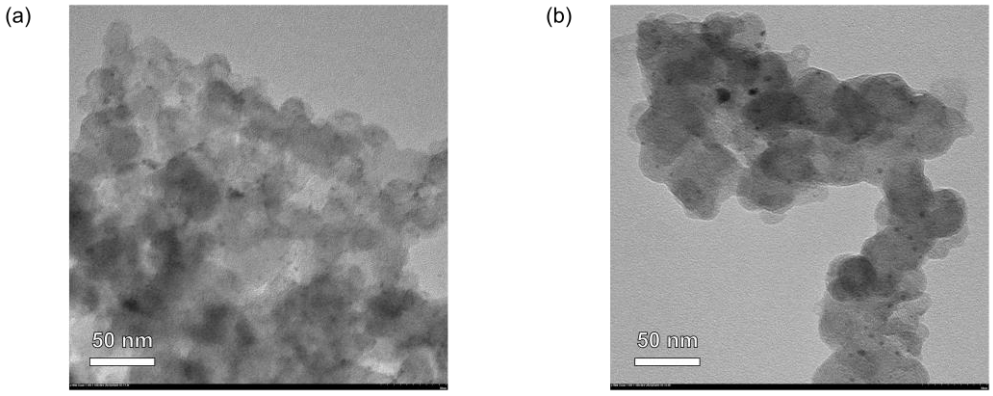

Fig. S3 TEM images of (a) PNPs/C and (b) In–PGM HEI NPs/C. Both images are displayed at the same magnification.

PXRD

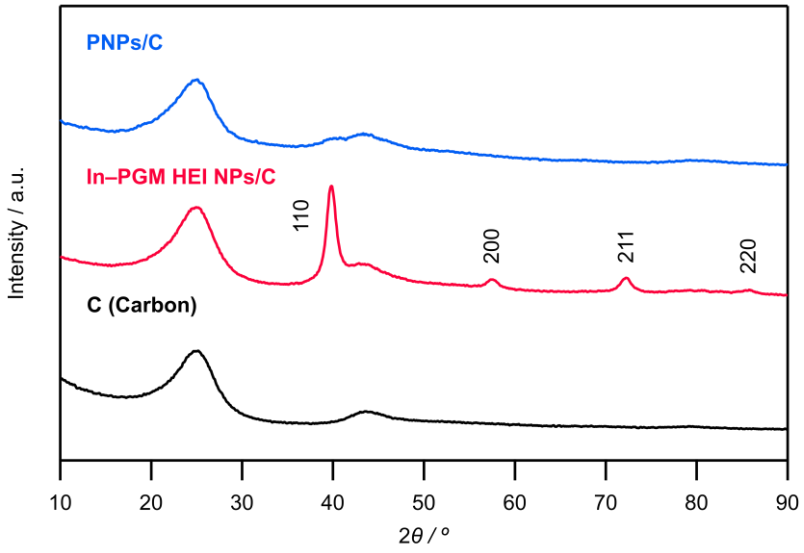

Fig. S4 PXRD profiles of PNPs/C, In–PGM HEI NPs/C and the carbon support (Cu*K*α, RT).

▼STEM observation of PNPs/C and In–PGM HEI NPs/C

Atomic-resolution STEM

The NPs were observed by STEM to obtain direct evidence of their crystal structure and particle size. For both the PNPs/C and In–PGM HEI NPs/C, crystalline parts represented in regular lattice images and amorphous parts without regular lattice images were found. The atomic arrangement and lattice constants of the crystalline parts were estimated based on *d*-spacings found in the atomic-resolution HAADF-STEM images. The *d*-spacing values were determined by fast Fourier transformation analysis.

PNPs/C was mostly composed of crystalline particles covered with amorphous oxides, plausibly ascribed to the metallic NPs covered with indium-rich oxide clusters. The crystalline parts were found to have an fcc structure. The estimated lattice constant was 3.9 Å, consistent with the value estimated by the Rietveld refinement. The typical particle size was about 2 nm, also consistent with the PXRD results.

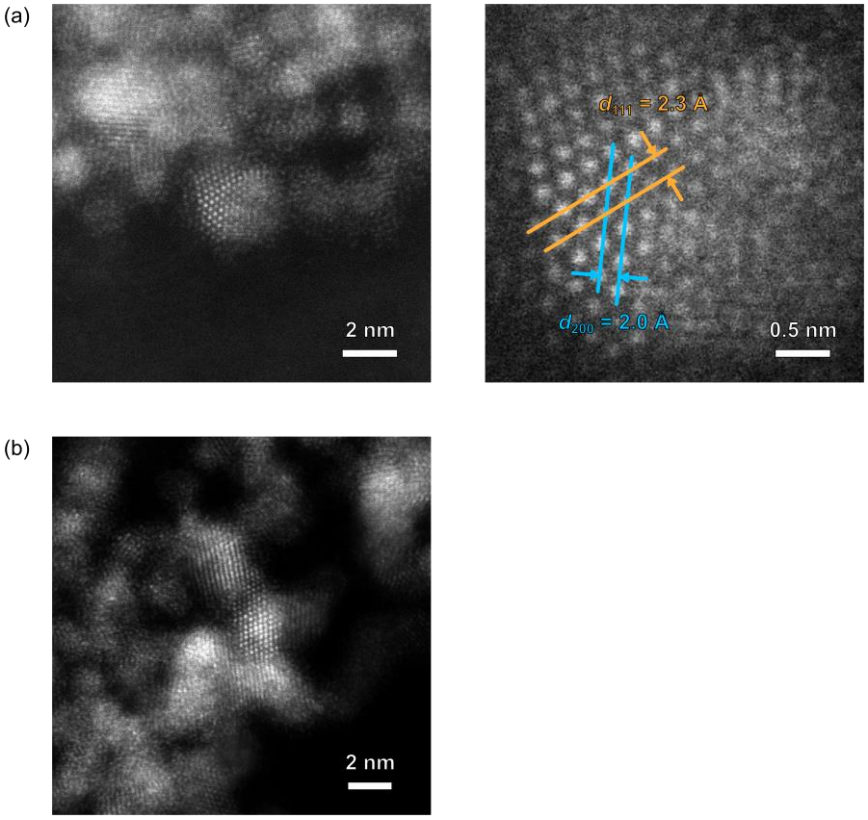

Fig. S5 HAADF-STEM images of PNPs/C in different fields of view (a) and (b). In the centre of (a), crystal viewed along the [110] axis can be found. The left figures show the whole NP to describe their sizes or environment, and the right figure shows the enlarged view to illustrate the *d*-spacings.

Although In–PGM HEI NPs/C still had some of the amorphous oxide clusters, B2 structured NPs that were never found in PNPs/C were found here. The estimated lattice parameter was 3.2 Å and the particle sizes were more than 5 nm.

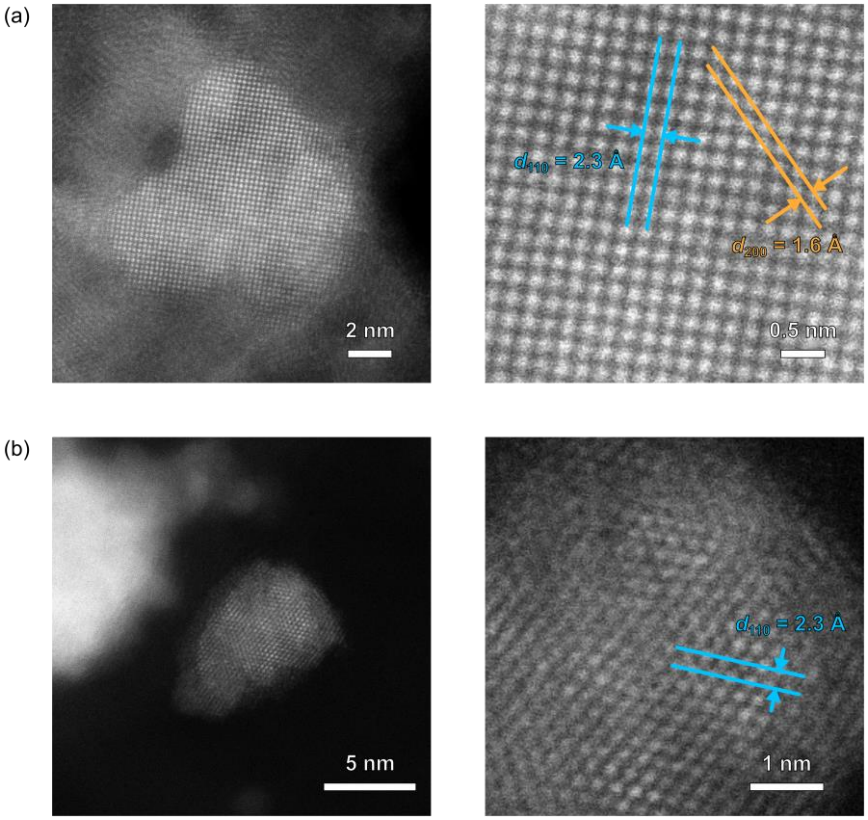

Fig. S6 HAADF-STEM images of In–PGM HEI NPs/C. The images show the B2-structured crystals viewed along (a) the [100] axis and (b) the [111] axis. The left images show whole NPs to describe their sizes or environment, and the right figures show enlarged views to illustrate the *d*-spacings.

Atomic-resolution EDX analysis

Atomic-resolution EDX analysis was performed targeting the B2-structured crystal viewed from the [100] axis. For clarity, the spatially resolved data were smoothed in a kernel size of three. The two-dimensional maps are shown in Fig. 2 in the main article and Fig. S7 below, and the one-dimensional line profile is shown in Fig. 3. Both show the distribution of indium and PGMs avoiding each other, supporting the ordered structure like the one shown in Figs. 2b and S7c.

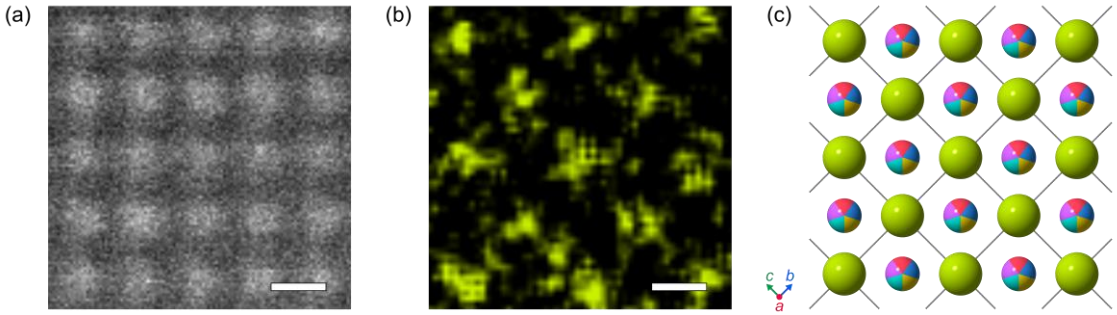

Fig. S7 Enlarged images of Fig. 2. (a) HAADF-STEM image, (b) EDX map of In *L* line net counts (contrast is enhanced compared with Fig. 2c for clarity) and (c) the crystal structure model from the same view. The scale bars in (a) and (b) represent 2 Å. In (c), green atoms represent indium and colourful atoms represent any one of the PGMs.

EDX analysis on PNPs

STEM-EDX analysis was also performed on PNPs (Fig. S8 and S9). The EDX map of In *L* line shows wider distribution than those of PGMs, supporting that the surface layer found in TEM images (Fig. S2) would be indium-rich oxide.

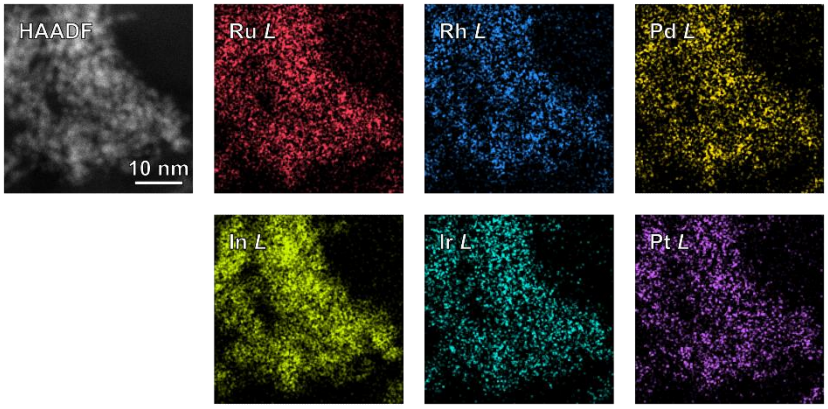

Fig. S8 HAADF-STEM image and EDX maps of PNPs.

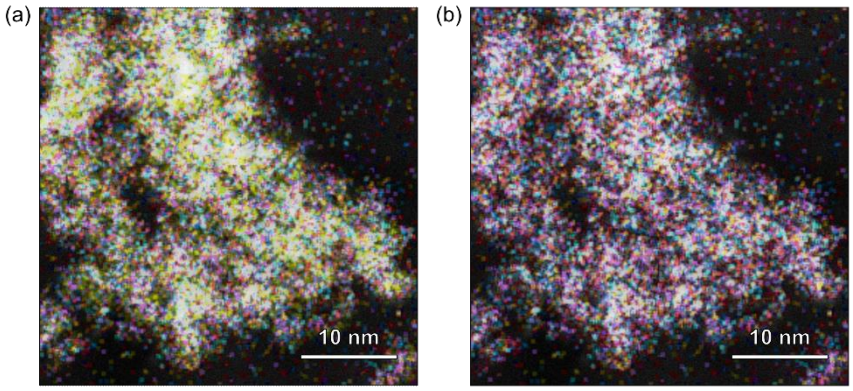

Fig. S9 Overlay of EDX maps of (a) all the metal elements and (b) all the PGMs. The same colours are attributed to each element as in Fig. S8.